

Fingerprinting the Electronic Wavefunctions of Ultra-Small Conductors

Gustavo A. Narvaez* and George Kirczenow

Department of Physics, Simon Fraser University, Burnaby, British Columbia, Canada V5A 1S6

(Dated: November 1, 2018)

By extending the Orthodox theory of Coulomb blockade to include the nano-scale effects of environmental electric fields, we show that tunneling spectra of metallic nanoislands contain information not only on the energies of the electronic levels but also on their *wavefunctions* near the surface of the island. This fundamental additional information is predicted to take the form of new observable phenomena beyond the scope of standard Orthodox theory: the tunneling resonances are renormalized and show surprisingly strong Gaussian fluctuations, level bending and avoided crossings.

PACS numbers: 73.22.Dj

I. INTRODUCTION

The Orthodox theory of Coulomb blockade¹ is a cornerstone of the present understanding of charge transport in single-electron devices^{2,3}. In this theory the device (a small metal, semiconductor or fullerene island and electrodes) is modeled using an equivalent electric circuit with macroscopic components (capacitors and resistors). Electronic interactions that control the passage of charge through the island are accounted for classically by an electrostatic *charging* energy U_c . The quantum nature of the island is incorporated through the discreteness of its energy levels. The statistical properties of the electron wavefunctions and energy levels are usually described within the frame of random matrix theory^{4,5,6} or by exact diagonalization of a microscopic Hamiltonian⁷. The average energy level separation δ and U_c set the energy scales of the transport problem. The Orthodox theory works impressively well for mesoscopic islands. Nevertheless, recently, a new generation of nanoscopic metallic islands (*nanoislands*) has yielded surprising tunneling spectroscopy results^{8,9,10,11} which have led theoreticians to extend the Orthodox theory in order to successfully account^{12,13,14,15} for some of the novel observations.

In this paper, the Orthodox theory is extended further in order to explore the microscopic effects of environmental electric fields on the tunneling spectroscopy of these nanoislands. These effects are due to penetration of the fields into the island, therefore they become more significant as the size of the island is reduced. To our knowledge they have not been considered previously in the experimental or theoretical literature. Our paradigm for studying them will be the transistor introduced by Ralph, Black and Tinkham¹¹, although environmental fields should affect all nanoscopic single-electron transistors. We show that environmental fields result in an *electrostatic renormalization* of the electronic states of the nanoisland that is beyond the scope of the standard Orthodox theory. This renormalization exhibits nearly-Gaussian fluctuations due to the stochastic nature of the electron wavefunctions. Furthermore, we predict the occurrence of avoided crossings and level bending due to the coupling between electronic levels induced by the fields. We show that these phenomena are reflected directly in

the behavior of tunneling resonances; this establishes a platform for probing the environmental coupling experimentally. The fluctuations in the slopes of the tunneling resonances vs. gate voltage that we predict are surprisingly strong, comparable in size to the unrenormalized slope predicted by Orthodox theory. We demonstrate that by observing these fluctuations it is possible to assess the amplitudes of the electronic wavefunctions at the surface of an ultra-small conductor. Moreover, the statistics of the wavefunctions at the surface of the nanoparticle can be separated from those in the bulk and measured. No way to measure these important properties of nanoparticle electron wave functions has been known until now. We conclude that a novel fingerprint of the electron wavefunctions at the surfaces of nanoscopic conductors can be found in tunneling spectroscopy experiments.

II. ENVIRONMENTAL ELECTRIC FIELDS

We now introduce the environmental electric fields. The model geometry¹¹ is shown in Fig. 1(a): Three macroscopic electrodes labeled $i = L$ and R (the source and drain contacts) and G (the gate), are separated from the central nanoisland (P) by thin insulating layers of thickness d^i , and are connected to voltage sources V_L , V_R , and V_G which drive the island to a potential $V_P = (C_\Sigma)^{-1} [Q_P - (C_L - C_R)V/2 + C_G V_G]$ in the Orthodox theory. Q_P is the charge on the nanoisland. C_L , C_R , and C_G are capacitances between electrode i and the nanoisland, and $C_\Sigma = C_L + C_R + C_G$. $V = V_R - V_L$ is the bias voltage with $-V_L = V_R = V/2$. The difference between V_i and V_P sets an electric field at the nanoisland surface (Ω_i) that faces electrode i . The electric field has a finite penetration depth (d_s) into the conductor (in the standard Orthodox model $d_s = 0$) that causes the electrostatic potential within the nanoisland to deviate from V_P . This deviation ($\Delta V_z^i = V_z^i - V_P$) is sketched in Figure 1(b). Assuming that the electric field within the metal nanoisland is screened exponentially¹⁶, ΔV_z^i at a distance z along the direction normal to Ω_i can be estimated as $\Delta V_z^i = \alpha_i (\lambda d^i + 2)^{-1} (V_i - V_P) e^{-\lambda z}$.¹⁷ $\alpha_i = \epsilon (\lambda d^i + 2) / (\lambda d^i + 2\epsilon)$ is a polarization enhancement

factor, where ϵ is the dielectric constant of the insulating material, and $\lambda = 1/d_s$ ($\simeq 1\text{\AA}^{-1}$ for Al¹⁸). Due to the effective screening (small d_s) in metals, only atoms near the surface are significantly perturbed by the electrostatic potential energy $\mathcal{U} = -e \sum_i \Delta V_z^i$.¹⁹ However, in the *nanoscopic* regime the substantial surface-to-volume ratio ($N_\Omega/N_V \sim 1$) of the nanoisland warrants the inclusion of \mathcal{U} in the calculation of its electronic structure. \mathcal{U} causes what we call the *microscopic electrostatic renormalization* of the energy levels, that is not included in the standard Orthodox theory. This renormalization is *in addition* to the *bulk* or *macroscopic* one due to $-eV_P$ that is included in the standard Orthodox theory.

III. RESULTS AND DISCUSSION

We begin by exploring the effects of \mathcal{U} analytically within perturbation theory. We then present results of

our *non-perturbative* computer simulations that apply to specific real systems: Al nanoislands with oxide tunnel barriers.

A. Perturbation theory in \mathcal{U}

We define the *microscopic* contribution to the energy $\mathcal{E}_a^q(V, V_G)$ of level $|\psi_a\rangle$ to be $\varepsilon_a^q(V, V_G)$, where $q = Q_P/e$ labels the charge state of the nanoisland. Let $|\psi_a^0\rangle$ be an electronic eigenstate for $V_G = 0$. For $V_G \neq 0$ these states become *coupled*: $\mathcal{U}_{ab} = \langle \psi_a^0 | \mathcal{U} | \psi_b^0 \rangle \neq 0$. Now suppose the coupling strength $\gamma_{ab} = \mathcal{U}_{ab} / [\mathcal{E}_a^0(0, 0) - \mathcal{E}_b^0(0, 0)]$ is small for all $|\psi_b^0\rangle$. Then, to first order in \mathcal{U} , (setting for simplicity $V = q = 0$) $\varepsilon_a^0(0, V_G)$ is *linear* in V_G with slope (see Appendix A)

$$S_a^m = \delta \varepsilon_a^0(0, V_G) / (e \delta V_G) = -(C_G/C_\Sigma) \sum_j |\psi_a^0(j)|^2 \left[-\alpha_L (\lambda d^L + 2)^{-1} e^{-\lambda z_j^L} - \alpha_R (\lambda d^R + 2)^{-1} e^{-\lambda z_j^R} + (C_\Sigma/C_G - 1) \alpha_G (\lambda d^G + 2)^{-1} e^{-\lambda z_j^G} \right], \quad (1)$$

where $|\psi_a^0(j)|^2$ is the amplitude of $|\psi_a^0\rangle$ at atomic site j of the nanoisland. z_j^i is the distance of site j from the surface Ω_i . Because d_s is smaller than the size of the nanoisland the leading terms in the summations correspond to atomic sites on the surfaces Ω_i . The surface of the nanoisland presents atomic scale disorder. Consequently, in the absence of magnetic fields, the electronic structure is described by the Gaussian orthogonal ensemble of random matrix theory^{5,7}. Therefore, $|\psi_a^0(j)|^2$ is a random variable that obeys a χ^2 distribution⁶. Thus the slope S_a^m *fluctuates* from state to state²⁰ reflecting the microscopic details of the electron wavefunctions at the surfaces of the nanoisland. Due to the form of Eq. (1) the fluctuations are nearly-Gaussian according to the central limit theorem. These observations remain valid for arbitrary V and q . We conclude from this analysis that the microscopic effects of the environmental electric fields lead to a fluctuating renormalization (*microscopic electrostatic renormalization*) of the electronic levels of a conducting nanoisland. It should be noted that in the standard Orthodox model ($d_s = 0$) S_a^m is zero.

Consider now the implications of this microscopic effect for the tunneling spectroscopy of the nano-

transistors. Suppose $Q_P = 0$ at $V = 0$ and fixed V_G , and then, after increasing the bias, an electron tunnels in from electrode L ($L \rightarrow P$) so that $Q_P = -e$. If $|\psi_a\rangle$ is being populated by the tunneling electron the transition is favorable only if the final state energy of the electron is lower than \mathcal{E}_F , the Fermi energy of electrode L : $\mathcal{E}_F \geq \mathcal{E}_a^-(V, V_G) = \varepsilon_a^-(V, V_G) + U_c - [(C_R + C_G/2)/C_\Sigma]eV - (C_G/C_\Sigma)eV_G$, where $U_c = e^2/2C_\Sigma$ is the charging energy¹. (Note that the *macroscopic* renormalization due to Q_P (through U_c), V and V_G constitutes the Orthodox model.) A similar restriction applies to tunneling transitions from the neutral nanoisland to electrode R . These conditions for tunneling set the threshold biases (V^{th}), the minimum values of V that satisfy them for a given $|\psi_a\rangle$. As V is swept at fixed V_G , each time a new V^{th} is reached a peak (a threshold resonance (*TR*)) appears in the differential conductance dI/dV ²⁴. We now analyze the effect of V_G on the *TR*, focusing on $L \rightarrow P$ transitions. In the perturbative regime we find (see Appendix B)

$$\frac{\delta V_{L \rightarrow P}^{th}(V_G)}{\delta V_G} = -\frac{C_G}{C_R + C_G/2} \{1 + S_a^m (-C_G/C_\Sigma)^{-1} - J_a^m [-(C_R + C_G/2)/C_\Sigma]^{-1} + \dots\}, \quad (2)$$

where $J_a^m = \delta\varepsilon_a^-(V, V_G)/(e\delta V)^{21}$. Equation (2) shows that the positions of the resonances in the dI/dV spectrum shift linearly with V_G . The first term on the right in Eq. (2) is the (*macroscopic*) slope predicted by standard Orthodox theory¹⁵; the other terms are due to microscopic effects. This analysis shows that the expected *macroscopic* slope of the *tunneling resonances* is *microscopically* renormalized. Furthermore, the slope of each resonance in the spectrum is different as a consequence of the *fluctuations*. Therefore it should be possible to study the coupling of the nanoisland's electronic levels to the environment by tunneling spectroscopy, and thus obtain experimental information on the electron wavefunction.

B. Non-perturbative computer simulations

So far our exposition, although perturbative, has been general. To understand the effects of the electric fields on the electronic structure and tunneling spectroscopy *beyond perturbation theory*, we now consider Al nanoislands coated with Al-oxide within a tight-binding model⁷ with the on-site orbital energies of the isolated neutral Al/Al-oxide nanoisland adapted to include \mathcal{U} . The presence of the oxide coating introduce surface disorder in these nanoislands, as explained in Ref. 7 (see also Ref. 22). We consider disc-shaped nanoislands of volume $\mathcal{V} \simeq 17nm^3$, and $d^R = 10\text{\AA}$, $d^L = 15\text{\AA}$ and $d^G = 4d^L$.²³ The latter choice assures that tunneling from the gate is suppressed. The parameters for two such systems are shown in Table I. The Fermi energies of the neutral isolated nanoislands (E_F^0) differ due to their differing structural disorder and geometries. The latter are also responsible for the differing capacitances. The *charging* voltage $V_U = e/C_\Sigma$ is the upwards (downwards) shift of V_P as one electron is removed (added) from (to) the nanoisland; the *degeneracy* gate voltage $V_G^\pm = \pm e/(2C_G)$ is, within the standard Orthodox theory¹, the value of V_G at which an electron is added (+) to or removed (-) from the nanoisland at $V = 0$.

Figure 2 shows results of the exact diagonalization of the tight binding Hamiltonian for $\varepsilon_a^q(V, V_G)$ for a few energy levels of transistors *A* and *B* under different bias and gate conditions, at $q = 0$. V_G ranges from approximately V_G^- to V_G^+ . V lies within the first step of the Coulomb staircase (at $V_G = 0$) of the nanoisland. Let us first focus on the effects of V_G at $V = 0$. The striking features are: i) *fluctuating* renormalization of the slopes of the energy levels due to the applied electric field, ii) linear dependence of some energy levels on V_G , and iii) level bending and avoided crossings with increasing $|V_G|$. These features are qualitatively similar regardless the values of q or V (not shown). We now proceed to discuss them. i) and ii) can be understood within the perturbative argument presented above. Regarding iii) it should be noted that as $|V_G|$ increases significant enhancement of γ_{ab} can occur due to increased coupling between levels and level proximity induced by V_G . In this case, the

microscopic contribution to the energy levels should be calculated to higher order in \mathcal{U} . Level bending signals the response of the energy levels to this change in the electronic coupling. As $|V_G|$ increases some energy levels become nearly degenerate. Since these levels are in general mixed by \mathcal{U} this results in avoided crossings in the spectrum. Thus level bending and avoided crossings as a function of gate bias should be general features of the spectra of these nano-transistors: Electric fields should effectively couple quasi-particle levels (which may even involve electronic excitations) that belong to the same Hilbert space *and* whose wavefunctions are such that the strength parameter γ_{ab} is significant. The microscopic effect of the source-drain voltage V on the electronic structure is also shown in Fig. 2 (for $q = V_G = 0$); there are again fluctuations and avoided crossings. These features are similar for finite values of q and V_G (not shown). The renormalization as a function of V , however, is smaller than for V_G due to the electrode geometry.

In conclusion, we have shown that the electronic levels are sensitive to the environmental electric fields and different regimes can be identified depending on the strength of the electric coupling between levels. The novel effects are predicted to occur in realistic Al/oxide transistors at the meV scale (see Fig. 2) that is readily accessible experimentally.

We now discuss the fluctuations of the slopes using the calculated $\varepsilon_a^0(V, V_G)$. Table I shows the average value (\mathcal{S}) of the slopes S_a^m , taken over $n = 101$ consecutive levels distributed symmetrically with respect to E_F^0 , and the Orthodox slope $-C_G/C_\Sigma$ for comparison. \mathcal{S} for transistor *A* is greater than for *B* by a factor of 1.34. This is consistent with Ω_G being 1.38 times bigger in *A* than in *B* (see Table I) and, consequently, more atomic sites being perturbed by the gate electric field. The standard deviation (σ) of S_a^m is roughly *equal* ($\simeq 2.3 \times 10^{-3}$) for the two transistors. Figure 3 shows the histograms for S_a^m in units of $-C_G/C_\Sigma$. The *microscopic* slopes of the energy levels are clearly significant fractions of the *macroscopic* slope arising from the Orthodox model. Indeed, for *B* the *microscopic* and the *macroscopic* effects are roughly equal. Thus the microscopic effects of environmental fields on the electronic structure and tunneling resonances that we have derived here can be a *very* important correction to macroscopic effects predicted by standard Orthodox theory. Both distributions in Fig. 3 are nearly Gaussian (the smooth lines in Fig. 3 are $n\Delta s(\sigma\sqrt{2\pi})^{-1} \exp[-(S_a^m - \mathcal{S})^2\sigma^{-2}/2]$, $\Delta s = 2 \times 10^{-3}$ is the bin size), as predicted from Eq. (1). The inset of Fig. 3 shows J_a^{m21} in units of $J_0 = -(C_R + C_G/2)/C_\Sigma$. Clearly, this effect is negligible when compared with S_a^m . Therefore, experimental measurements of $\delta V^{th}/\delta V_G$ can accurately determine S_a^m and hence the microscopic effects of the environmental fields on the nanoisland energy levels; see Eq. (2).

IV. SUMMARY

In summary, we have shown that coupling to environmental electric fields gives rise to a unique fingerprint of the electron wavefunction at the surface of a nanoscopic conductor that can be observed in tunneling experiments. While we illustrated this by considering Al/Al-oxide nanoislands our findings rely only on the ability of ultrasmall *conducting* islands to screen electric fields, and their large surface-to-volume ratio. Therefore, other metallic nanoislands (noble and magnetic) and more exotic nanoscopic conductors such as metallic carbon nanotubes²⁵ may also reveal the fingerprints of their electron wavefunctions. We hope our results will motivate experimentalists to look for these fingerprints.

Acknowledgments

We thank John W. Wilkins for his helpful comments. This research was funded by the Natural Science and Engineering Research Council of Canada (NSERC) and the Canadian Institute for Advanced Research (CIAR).

APPENDIX A: DERIVATION OF EQ. (1)

In Section II we showed that the applied bias (V) and gate (V_G) voltages drive the nanoisland to a potential V_P that depends on the charge state (Q_P) of the nanoisland, and the values of V and V_G . Applying *only* V_G to a neutral nanoisland results in $V_P = (C_G/C_\Sigma)V_G$. In this case ($V = Q_P = q = 0$), the electrostatic potential energy \mathcal{U} is given by:

$$\mathcal{U} = -eV_G(C_G/C_\Sigma) \left[-\alpha_L(\lambda d^L + 2)^{-1}e^{-\lambda z_j^L} - \alpha_R(\lambda d^R + 2)^{-1}e^{-\lambda z_j^R} + (C_\Sigma/C_G - 1)\alpha_G(\lambda d^G + 2)^{-1}e^{-\lambda z_j^L} \right] \quad (\text{A1})$$

Note that Eq. (A1) becomes *different* for other Q_P , V , and V_G values.

Within first order perturbation theory in \mathcal{U} , the microscopic contribution to the energy $\mathcal{E}_a^0(0, V_G)$ of level $|\psi_a\rangle$, $\mathcal{E}_a^0(0, V_G)$, is:

$$\begin{aligned} \mathcal{E}_a^0(0, V_G) &= \mathcal{E}_a^0(0, 0) + \langle \psi_a^0 | \mathcal{U} | \psi_a^0 \rangle \\ &= -eV_G(C_G/C_\Sigma) \sum_j |\psi_a^0(j)|^2 \left[-\alpha_L(\lambda d^L + 2)^{-1}e^{-\lambda z_j^L} - \alpha_R(\lambda d^R + 2)^{-1}e^{-\lambda z_j^R} \right. \\ &\quad \left. + (C_\Sigma/C_G - 1)\alpha_G(\lambda d^G + 2)^{-1}e^{-\lambda z_j^L} \right] \end{aligned} \quad (\text{A2})$$

where $|\psi_a^0\rangle$ is an electronic eigenstate for $V_G = 0$, as mentioned in the text (Sec. III A), and the summation is performed over all atomic sites.

Equation (1) in the text is straight forwardly derived from Eq. (A2).

APPENDIX B: DERIVATION OF EQ. (2)

As discussed in the text (Sec. III A), $V_{L \rightarrow P}^{th}(V_G)$ is the minimum (threshold) value of the bias voltage—in the presence of an applied gate voltage V_G —at which an electron tunnels from electrode L into an empty state $|\psi_a\rangle$ in the nanoisland (P). This threshold value is given by:¹

$$\mathcal{E}_F = \varepsilon_a^-(V_{L \rightarrow P}^{th}(V_G), V_G) + U_c - [(C_R + C_G/2)/C_\Sigma]eV_{L \rightarrow P}^{th}(V_G) - (C_G/C_\Sigma)eV_G. \quad (\text{B1})$$

After a simple manipulation, Eq. (B1) leads to:

$$\frac{\delta V_{L \rightarrow P}^{th}(V_G)}{\delta V_G} = -\frac{C_G}{C_R + C_G/2} \left\{ 1 + (-C_G/C_\Sigma)^{-1} \left[\frac{\varepsilon_a^-(V_{L \rightarrow P}^{th}(V_G + \delta V_G), V_G + \delta V_G) - \varepsilon_a^-(V_{L \rightarrow P}^{th}(V_G), V_G)}{e\delta V_G} \right] \right\} \quad (\text{B2})$$

Then, we calculate within first order perturbation theory in \mathcal{U} (setting $Q_P = -e$ and taking V and V_G as variables) the values of $\varepsilon_a^-(V, V_G)$. The latter leads to the following identity:

$$\frac{\varepsilon_a^-(V_{L \rightarrow P}^{th}(V_G + \delta V_G), V_G + \delta V_G) - \varepsilon_a^-(V_{L \rightarrow P}^{th}(V_G), V_G)}{e\delta V_G} = \delta\varepsilon_a^-(V, V_G)/(e\delta V_G) = S_a^m + J_a^m \left(\frac{\delta V_{L \rightarrow P}^{th}(V_G)}{\delta V_G} \right) \quad (B3)$$

where $J_a^m = \delta\varepsilon_a^-(V, V_G)/(e\delta V)$. By combining Eqs. (B2) and (B3) we get:

$$\frac{\delta V_{L \rightarrow P}^{th}(V_G)}{\delta V_G} = -\frac{C_G}{C_R + C_G/2} [1 + S_a^m (-C_G/C_\Sigma)^{-1}] \{1 + J_a^m [-(C_R + C_G/2)/C_\Sigma]^{-1}\}^{-1} \quad (B4)$$

Finally, by expanding the denominator of Eq. (B4) in powers of $J_a^m [-(C_R + C_G/2)/C_\Sigma]$ we obtain Eq. (2).

- * Present address: Department of Physics, The Ohio State University, Columbus, Ohio 43210
- ¹ I. O. Kulik and R. I. Shekhter, Zh. Eksp. Teor. Fiz. **62**, 623 (1975) [Sov. Phys. JETP **41**, 308 (1975)]; K. K. Likharev, IBM J. Res. Dev. **32**, 144 (1988); Proc. IEEE **87**, 606 (1999); D. V. Averin and A. N. Korotkov, Zh. Eksp. Teor. Fiz. **97**, 1661 (1990) [Sov. Phys. JETP **70**, 937 (1990)]; D. V. Averin and K. K. Likharev, in *Mesoscopic Phenomena in Solids*, Eds. B. L. Altshuler, P. A. Lee, and R. A. Webb (Elsevier, Amsterdam, 1991); G.-L. Ingold and Yu. Nazarov, in *Single Charge Tunneling*, Eds. H. Grabert and M. H. Devoret, (Plenum, NY, 1991);
 - ² For reviews see: L. P. Kouwenhoven, D. G. Austing, and S. Tarucha, Rep. Prog. Phys. **64**, 701 (2001); Y. Takahashi, NTT Rev. **12**, 12 (2000); M. A. Kastner, Rev. Mod. Phys. **64**, 849 (1992)
 - ³ M. Ciorga, A. Wensauer, M. Pioro-Ladriere, M. Korkusinski, J. Kyriakidis, A. S. Sachrajda, and P. Hawrylak, Phys. Rev. Lett. **88**, 256804 (2002); J. Park, A. N. Pasupathy, J. I. Goldsmith, C. Chang, Y. Yaish, J. R. Petta, M. Rinkoski, J. P. Sethna, H. D. Abruña, P. L. McEuen, and D. C. Ralph, Nature **417**, 722 (2002); W. W. Liang, M. P. Shores, M. Bockrath, J. R. Long, H. Park, Nature **417**, 725 (2002). D. Goldhaber-Gordon, H. Shtrikman, D. Mahalu, D. Abusch-Magder, U. Meirav, M. A. Kastner, Nature **391**, 156 (1998)
 - ⁴ Y. Alhassid, Rev. Mod. Phys. **72**, 895 (2000); A. D. Mirlin, Phys. Rep. **326**, 260 (2000)
 - ⁵ K. B. Efetov, Adv. Phys. **32**, 53 (1983); W. P. Halperin, Rev. Mod. Phys. **58**, 533 (1986)
 - ⁶ T. A. Brody, J. Flores, J. B. French, P. A. Mello, A. Pandey, S. S. M. Wong, Rev. Mod. Phys. **53**, 385 (1981)
 - ⁷ G. A. Narvaez and G. Kirczenow, Phys. Rev. B **65**, 121403(R) (2002); *ibid* **66**, 081404(R) (2002)
 - ⁸ D. C. Ralph, C. T. Black, and M. Tinkham, Phys. Rev. Lett. **74**, 3241 (1995); C. T. Black, D. C. Ralph, M. Tinkham, Phys. Rev. Lett. **76**, 688 (1996); D. Davidović and M. Tinkham, Phys. Rev. Lett. **83**, 1644 (1999); Phys. Rev. B **61**, R16359 (2000); S. Guéron, M. M. Deshmukh, E. B. Myers, and D. C. Ralph, Phys. Rev. Lett. **83**, 4148 (1999); D. G. Salinas, S. Guéron, D. C. Ralph, C. T. Black, M. Tinkham, Phys. Rev. B **60**, 6137 (1999)
 - ⁹ J. R. Petta, D.C. Ralph, Phys. Rev. Lett. **87**, 266801 (2001).
 - ¹⁰ M. M. Deshmukh, S. Kleff, S. Guéron, E. Bonet, A. N. Pasupathy, J. v. Delft, D. C. Ralph, Phys. Rev. Lett. **87**, 226801 (2001); M. M. Deshmukh, E. Bonet, A. N. Pasupathy, D. C. Ralph, Phys. Rev. B **65**, 073301 (2002)
 - ¹¹ D. C. Ralph, C. T. Black, and M. Tinkham, Phys. Rev. Lett. **78**, 4087 (1997)
 - ¹² O. Agam, N. S. Wingreen, B. L. Altshuler, D. C. Ralph, and M. Tinkham, Phys. Rev. Lett. **78**, 1956 (1997)
 - ¹³ P. W. Brouwer, X. Waintal, and B. I. Halperin, Phys. Rev. Lett. **85**, 369 (2000); K. A. Matveev, L. I. Glazman, and A. I. Larkin, Phys. Rev. Lett. **85**, 2789 (2000)
 - ¹⁴ A. H. MacDonald, C. M. Canali, Solid State Comm. **119**, 253 (2001); C. M. Canali and A. H. MacDonald, Phys. Rev. Lett. **85**, 5623 (2000); S. Kleff, J. v. Delft, M. M. Deshmukh, and D. C. Ralph, Phys. Rev. B **64**, 220401(R) (2001); I. L. Aleiner, P. W. Brouwer and L. I. Glazman, Phys. Rep. **358**, 309 (2002); E. Bonet, M. M. Deshmukh, and D. C. Ralph, Phys. Rev. B **65**, 045317 (2002)
 - ¹⁵ J. v. Delft and D. C. Ralph, Phys. Rep. **345**, 61 (2001)
 - ¹⁶ This assumption is justified within the Thomas-Fermi screening model. For details of this topic see: *Solid State Physics*, N. W. Ashcroft and N. D. Mermin (Saunders, 1976)
 - ¹⁷ The derivation of this expression is straight forward. It relies on (a) The assumption that the magnitude of the electric field deep inside the electrodes (L , R , and G) and the nanoisland is negligibly small and thus V_L , V_R , V_G , V_P are equal to the values of the electrostatic potential there; and (b) The use of appropriate boundary conditions for an electric field at the metal/dielectric (the insulating oxide layer that separates the nanoisland from the electrodes) interface. For details see: *Foundations of Electromagnetic Theory*, J. R. Reitz, F. J. Milford, and R. W. Christy (Adison-Wesley, 1979)
 - ¹⁸ D. M. Newns, Phys. Rev. B **1**, 3304 (1970)
 - ¹⁹ Note that \mathcal{U} depends on the charge state of the nanoisland (Q_P), applied bias (V) and gate (V_G) voltages.
 - ²⁰ The randomness of $|\psi_a^0(j)|^2$ is also responsible for the fluctuating g-factors of noble metal nanoislands^{9,13}.
 - ²¹ In the linear regime $J_a^m = \delta\varepsilon_a^-(V, 0)/(e\delta V)$. Our simulations show that this is a good approximation in general.
 - ²² We briefly mention here details regarding the amount and type of disorder present in our model Al/Al-oxide nanoislands. Further details may be found in Ref. 7. We first identify the atomic sites in the nanoisland that belong to the surface by looking at the number of nearest-neighbors

that a given site has. In the cases where this number is smaller than the coordination number in a face-centered-cubic lattice the atom is regarded as a surface atomic site. In our model, the surface atoms represent the metal/oxide interface—the oxide coating. Hence, these atoms are *randomly* assigned to be either oxygen or charged—due to oxidation—aluminum atoms. Here we assume for simplicity that equal numbers of atoms of the two species are present at the surface.

- ²³ These values of d^i are physically reasonable choices. Smaller values greatly *enhance* the microscopic effects.
- ²⁴ D. V. Averin and A. N. Korotkov in Ref. 1
- ²⁵ H. W. Ch. Postma, T. Teepen, Z. Yao, M. Grifoni, C. Dekker, *Science* **293**, 76 (2001); M. Bockrath, D. H. Cobden, P. L. McEuen, N. G. Chopra, A. Zettl, A. Thess, R. E. Smalley, *Science* **275**, 1922 (1997)

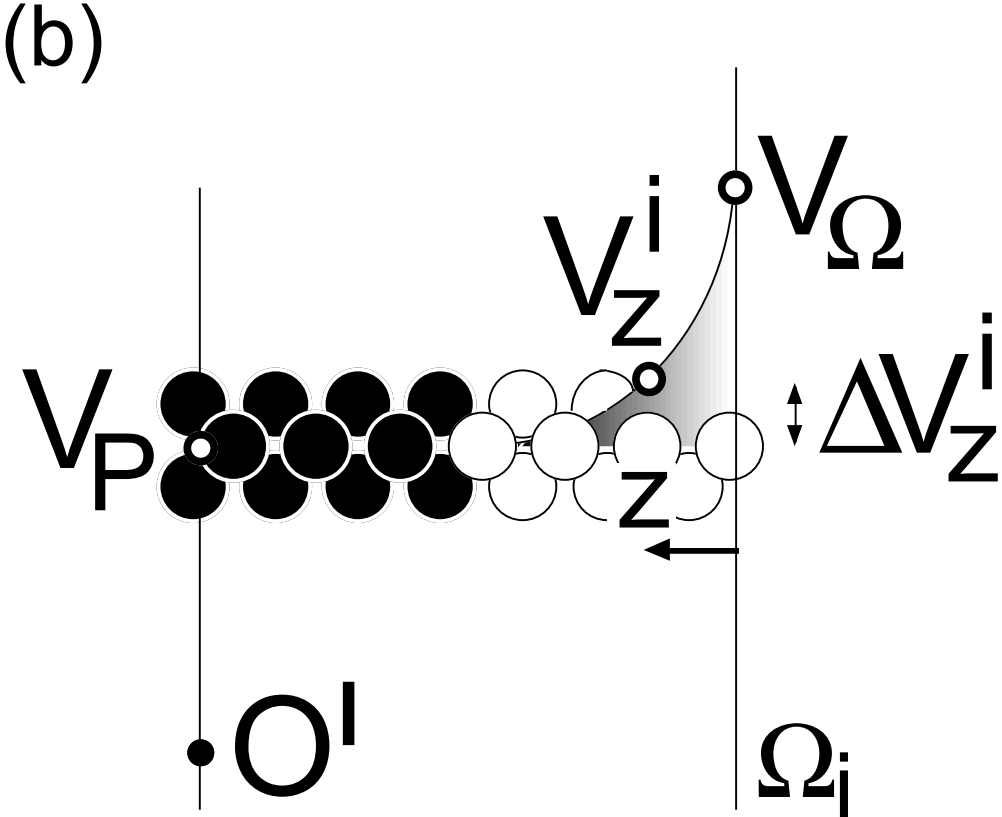
label	D (nm)	h (nm)	$N_{\Omega}/N_{\mathcal{V}}$	E_F^0 (eV)	C_R (aF)	C_L (aF)	C_G (aF)	e/C_{Σ} (mV)	$e/2C_G$ (mV)	\mathcal{S}	$-C_G/C_{\Sigma}$
A	3.646	1.62	0.774	8.289	1.480	1.057	0.164	59.32	488.47	-0.0214	-0.0607
B	5.266	0.81	1.045	8.281	3.088	2.206	0.109	29.65	734.95	-0.0159	-0.0202

TABLE I: Transistor parameters: Diameter (D), height (h), surface-to-volume ratio ($N_{\Omega}/N_{\mathcal{V}}$), Fermi energy of the neutral isolated grain (E_F^0), capacitances, and charging and degeneracy voltages. \mathcal{S} is the average slope due to microscopic renormalization and $-C_G/C_{\Sigma}$ is the Orthodox model slope (see text).

FIG. 1: (a) Schematic of the model transistors. The island (black and white circles) is disc-shaped and is *surrounded* by the gate (G). White circles indicate where environmental electric fields are important. (b) Sketch of the deviation ΔV_z within the island. O' indicates its center.

FIG. 2: Fingerprints of the electronic wave functions: microscopic contribution to the energy levels of the transistors vs. V_G (at $V = 0$) and V (at $V_G = 0$) with $Q_P = 0$. Voltages are in mV.

FIG. 3: Histograms (broken lines) of S_a^m in *units* of the standard Orthodox theory slope: $-C_G/C_{\Sigma}$. Gaussian distributions (smooth lines) corresponding to the calculated \mathcal{S} and σ (see text). Inset: Histograms of J_a^m in units of $J_0 = -(C_R + C_G/2)/C_{\Sigma}$ for A (bold line) and B (thin line).



(b)

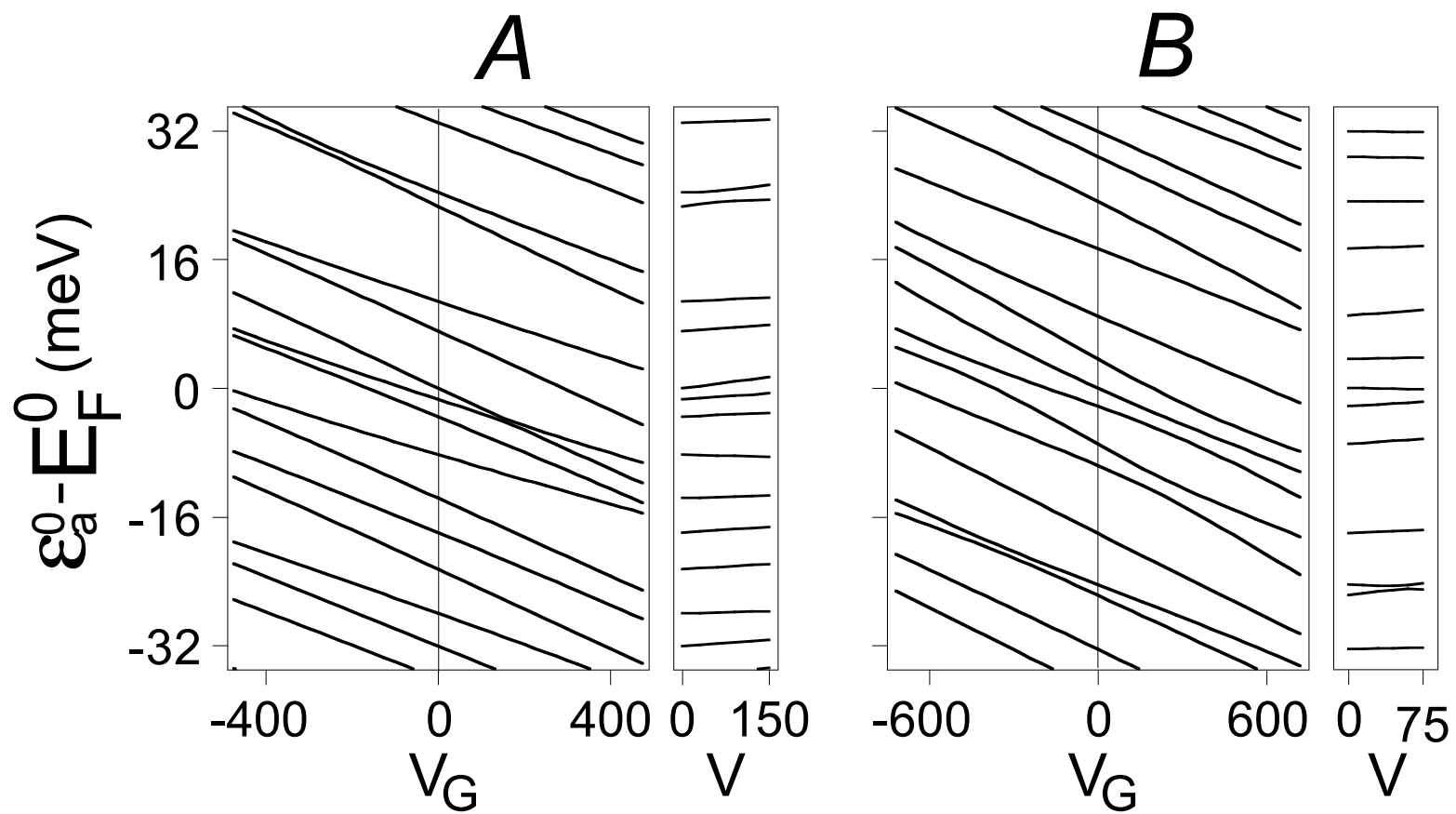


Figure 2, Narvaez and Kirczenow

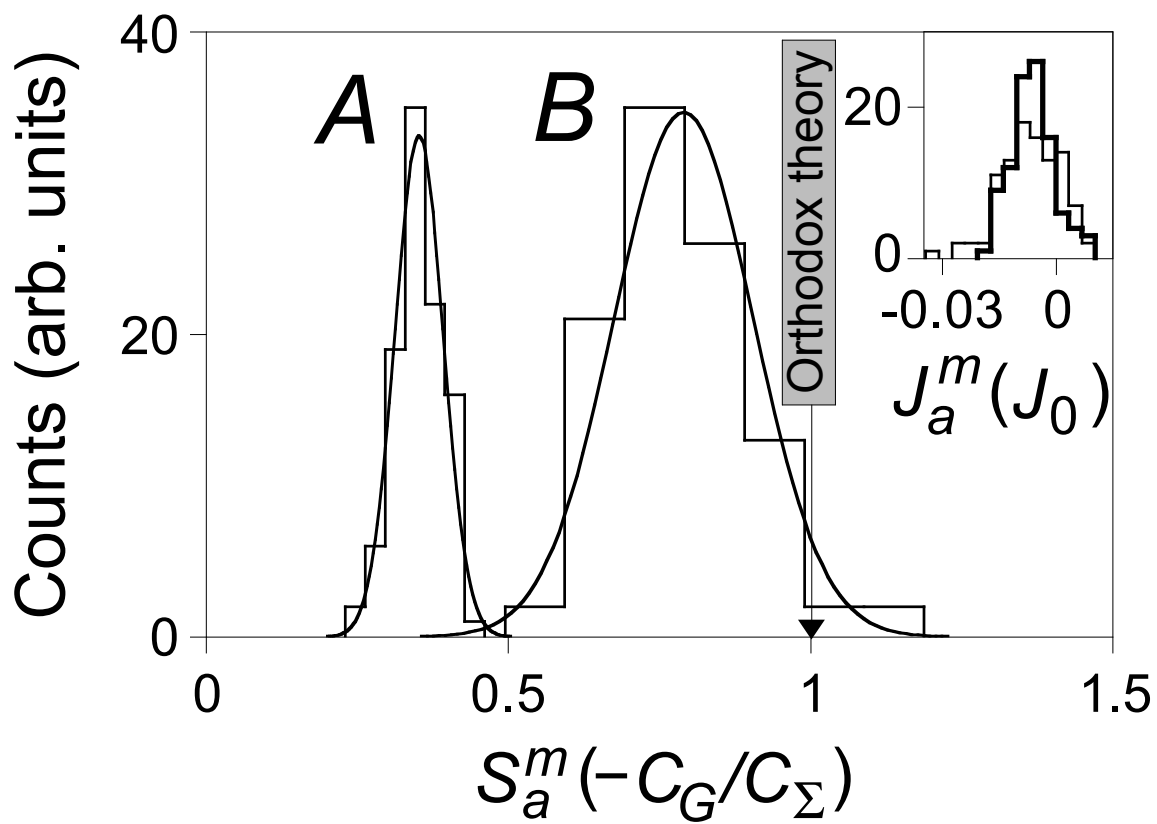


Figure 3, Narvaez and Kirczenow